2D and 3D Measurement Algorithms for Real Front and Back Curved Surfaces of Contact Lenses

Kentaro Saeki[1,2][a], Decai Huyan[2], Akira Nakamura[1], Shin Kubota[1], Kenji Uno[1,3],
Kazuhiko Ohnuma[1,3] and Tatsuo Shiina[2][b]

[1]SEED CO., LTD, 2-40-2 Hongo, Bunkyo-ku, Tokyo, Japan
[2]Graduate School of Science and Engineering, Chiba University 1-33 Yayoi-cho, Inage-ku, Chiba-shi, Chiba, Japan
[3]Laboratorio de Lente Verde, 98-1 Nozomino, Sodegaura, Chiba, 299-0251, Japan

Keywords: OCT, Vertical Incidence, Shape Measurement, Transparent Sample, Contact Lens.

Abstract: The 2D and 3D measurement algorithms for real front and back curved surfaces of contact lenses (CL) were developed. The purpose of 2D algorithm is to evaluate spherical lenses. We adopted the algorithm to be incident the probe light vertically along the curved surfaces of CLs under the condition that the difference of curvature radii between the front and back surfaces is small enough within numerical aperture (N.A.) of the optical probe. The vertical incidence against the curved surface is judged by using the intensity balance between OCT interference signals from both front and back surfaces of CL. As a result, the lens shape matched with the design value and RMSE of the thickness was 5.33 μm. Also, regarding the curvature radii, compatibility between this OCT device and the conventional device was indicated. In the 3D algorithm, we conducted a basic experiment using some special lenses in order to develop non-cylindrical lens measurement. By moving a 2-axis (vertical and horizontal) Micro Electro Mechanical System (MEMS) mirror with phase difference of 90°, it was designed to conduct circular scanning while maintaining vertical incidence of probe beam on the front surface of CL. The shape and the curvature radius was evaluated with simulation data under the same conditions. As a result, although it has an error against the design value, the result and the simulation result matched well.

1 INTRODUCTION

In contact lens (CL) manufacturing processes, it is essential to evaluate the shape of the transparent object (B. J. Coldrick 2016, D, Luo 2019). When measuring the refractive power of CL, non-contact measurement is critical and it is necessary to evaluate the following three elements that determine the refractive power: 1. Lens center thickness, 2. Curvature radius of the front and back surfaces and 3. Refractive index. In addition, at present, CL peripheral shape is emerging as an important issue for new design such as lenses for myopia control.

Shape measurement using a tool such as a contact gauge is limited because it is a single-sided shape measurement at the light incidence position. Also, with this contact gauge, only data of the central part is collected, the device provides no information regarding the shape from lens center to the peripheral part. Similarly, regarding the thickness of a CL, since the peripheral thickness is manually measured at only several points with a thickness gauge, it is difficult to know a thickness distribution of CL over a wide range. And regarding the conventional 3D measuring device, it needs to be measured by using a special antireflection so that the reflection from inside doesn't interfere with the measurement (F. Drouet 2014). In addition, even with a measuring device using a confocal method, when measuring the front surface of a thin CL, the back surface is sometime focused and it may affect the result (Saeki 2020). These are disadvantages of single-sided shape measurement. Their problems can be solved if simultaneous front and back measurement can be achieved. In addition, it is important for optical lens

[a] https://orcid.org/0000-0002-4902-3110
[b] https://orcid.org/0000-0001-9292-4523

73

evaluation because it can evaluate the misalignment of the both surfaces.

Optical Coherence Tomography (OCT) is a non-invasive and non-contact technology that has the advantages of high speed and high accuracy (Tanno 1990). It has been attracting a lot of attention from the ophthalmology industry in the medical field (P. Massatsch 2005). On the other hand, in the industrial field, although it is mainly used for thickness inspections (Hibino 2004, H. C. Cheng 2010), there are few reports about the application for measurement of shape. The reason for this is that the measurement sample is usually placed in the epi-illumination position. Therefore, since the back shape is greatly affected by the refractive index, it has not been used for shape measurement.

This study proposes two algorithms for accurately measurement of the real CL shape of the front and back surfaces with 2 dimensional and 3 dimensional methods. In 2D algorithm, spherical lenses were evaluated. We adopted the algorithm to be incident light vertically along the curved surfaces of CL under the condition that the difference of curvature radii between the front and back surfaces is small enough within numerical aperture (N.A.) of the optical probe. The vertical incidence against the curved surface is judged by using the intensity balance between OCT interference signals from both front and back surfaces of CL. On the other hand, in 3D algorithm, we conducted a basic experiment using some special lenses in order to develop non-cylindrical lens measurement. By controlling a 2-axis (vertical and horizontal) Micro Electro Mechanical System (MEMS) mirror with phase difference of 90°, it conducted circular scanning while maintaining vertical incidence of probe beam on the front surface of CL. In this design, as the drive angle can be changed by adjusting the voltage applied to the MEMS mirror, the measurement range can be changed. In this report, the shape, thickness, and curvature radius of the front and back surfaces of the transparent CL were evaluated using two algorithm.

2 EXPERIMENTAL SET-UP

2.1 TD-OCT Systems

In this study, Time-Domain (TD) OCT was adopted. It allows its optical probe design to have long working distance and wide measurement range (Shiina, 2003). The measurement probe can be designed independently from other parameters such as resolution, scanning speed and measurement range in

its specification. Furthermore, since the interference signal is magnified linearly, the linearity of the measured signal is high. Figure 1 shows a schematic diagram of this system. In addition, Table 1 shows the specifications of 2D and 3D system, respectively. The 2D's super luminescent diode (SLD) light is 1310nm. This is to measure the lens itself. In contrast, for 3D, SLD light 856nm was selected in consideration of the development of eyeball model for axial length measurement.
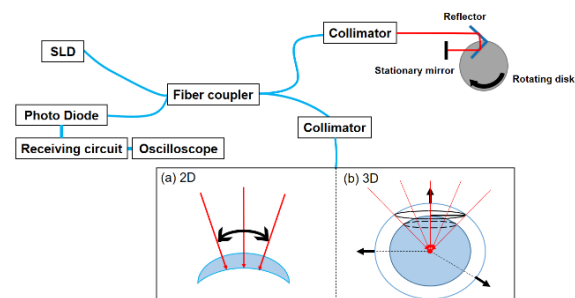

Figure 1: A schematic diagram for TD-OCT system. (a) is 2D and (b) is 3D.

Table 1: Specifications of TD-OCT measurement system.

Algorithm	Parts	Item	Specifications
2D	SLD	Wavelength	1310 nm
		Spectral Width	55 nm
		Resolution	13.8 μm
	Measurement stage	Position Accuracy	1 μm
		Rotation	15 scan/s (900rpm)
		Rotation Radius	15 mm
	N.A.		0.14
3D	SLD	Wavelength	856nm
		Spectral Width	32.1nm
		Resolution	10.1μm
	MEMS	Angular resolution	< 5 μrad
		Maximum scanning angle	±10 deg
		Drive frequency	< 450 Hz
		Drive voltage	-5 ∼ 5 V
	Cylindrical Lens	Focal length	200 mm
	Lens1	Focal length	100 mm
	Lens2	Focal length	40 mm
	N.A		0.015

2.2 2D Shape Measurement Algorithm

In this study, we propose a measurement algorithm which makes the incidence light always hits perpendicularly to front and back surfaces of a spherical CL to measure its real shapes. Figure 2 shows the measurement algorithm using the metal ball. The sample stage mechanism was designed so that its translation movement and vertical rotation can be changed in order to measure both front and back surfaces' interference echoes, which assume sign of the vertical incidence. In the Fig. 2, the dash line shows the initial position of the metal ball and the solid line shows the position where it is rotated on the vertical rotation angle and translated to get the vertically incidence position. The position of 2nd interference point (IP) is calculated by using the vertical rotation angle and translation.

The measurement data includes the translation distance d, the vertical rotation angle θ and the optical path positions of the front surface interference time t_1, and the back surface interference time t_2. The OCT interference times are converted into the distance using the reflector rotation speed. Then the distance is converted into the coordinates with the equation (1) - (4) using the vertical rotation angle and translation distance on this algorithm. In the case of CLs, two interference signals occur. The interval between them indicates the thickness. Since light passes through the substance, the group refractive index was taken into consideration for calculating the back surface coordinates. Equation (1) and (2) were used to calculate the front curvature coordinate, and (3) and (4) were used to calculate the back curvature coordinate.

$$x_f = d\cos\theta - a(t_{all} - t_1)\sin\theta \quad (1)$$

$$y_f = d\sin\theta + a(t_{all} - t_1)\cos\theta - e \quad (2)$$

$$x_b = d\cos\theta - a\{t_{all} - [t_1 + (t_2 - t_1)/n]\}\sin\theta \quad (3)$$

$$y_b = d\sin\theta + a\{t_{all} - [t_1 + (t_2 - t_1)/n]\}\cos\theta - e \quad (4)$$

a is a time-distance conversion coefficient which is calculated from the change of the optical path length depending on the rotation speed of the reflector. t_{all} is the optical path length (time unit) from the OCT measurement range origin to the center of CL rotation. n is the group refractive index of the CL. e is the difference in length between the center of the curvature radius and the center of the CL rotation. It was calculated by using a curvature radius of a known spherical metal ball. Then, the curvature

radius was estimated from the (x,y) coordinates by a circle approximation using the least-squares method.

For comparison with a conventional measurement device, a confocal laser microscope (Sensofar: Plu Apex) was adopted. Since it is single-sided shape measurement device, the CL was turned over to measure the shape of the back surface after measuring the front surface. The curvature radius was compared with the OCT result.
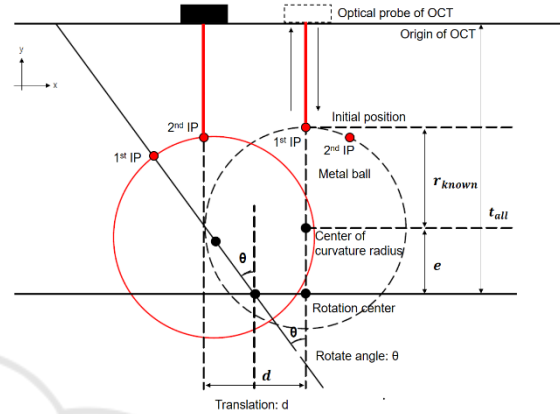

Figure 2: 2D measurement algorithm using the metal ball.

2.3 3D Shape Measurement Algorithm

In 3D algorithm, we conducted a basic experiment using some special lenses in order to develop a non-cylindrical lens measurement. In order to realize this algorithm, it was designed to conduct circular scanning by driving two MEMS mirror (Hamamatsu Photonics: 2D-OSE201) on the vertical and horizontal axes with a phase difference of 90°. Moreover, since this MEMS mirrors don't have a resonance frequency, the drive frequency can be changed, and the measurement angle can also be changed by the drive voltage. By using two MEMS mirrors, a cylindrical lens was used to correct the misalignment for each axis. The number of measurement points in this OCT system depends on the difference between the reflector rotation frequency f_1 of the variable optical path mechanism and the drive frequency f_2 of MEMS mirrors. Assuming that the minimum measurement point is 2n (n = 1, 2, 3,···), f_2 is calculated from equation (5) using f_1.

$$f_2 = \left(1 + \frac{1}{4n}\right)f_1 \quad (5)$$

In this measurement, firstly, the time difference t_1 between the trigger signal at focal position of the measurement probe and the OCT interference position was measured. And in the circular sannning,

the time difference t_1' is measured. Using these time differences, the distance r from the focal point of the measurement probe to each measurement point is estimated. In addition, in the MEMS mirrors, the time difference t_2 and t_3 between the driving singnals of MEMS mirror in the horizontal/vertical direction and the interference positions are defined, respectively. The incident angle θ and the vertical incident angle φ are calculated using t_2 and t_3. Three-dimensional coordinates (x, y, z) are caluculated from r, θ and φ using equation (6) – (8).

$$x = r \cos \theta \cos \varphi \qquad (6)$$

$$y = r \cos \theta \sin \varphi \qquad (7)$$

$$z = r \sin \theta \qquad (8)$$

After the coordinate conversion, the position (x, y, z) of each OCT inteference point were fitted by the least squares method of the sphere. Then, after applying the correction, the curvature radius and center coordinates were evaluated.
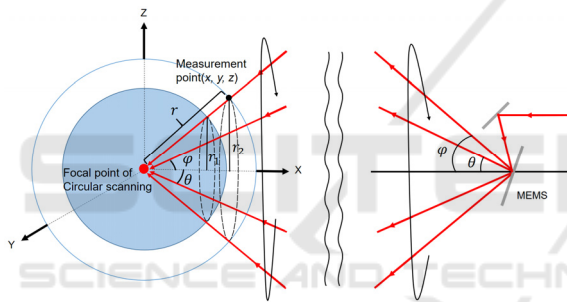

Figure 3: 3D measurement algorithm.

2.4 Measurement Sample

Rigid CLs were adopted as transparent samples. They were practically designed and specially manufactured for the purpose of this study. The refractive index of the material is 1.455 ± 0.02, which was measured with Abbe's refractometer (Atago: NAR-1T SOLID). The curvature radii of both front and back surfaces were manually measured with a contact gauge (NEITZ: CGX-3). A typical CL structure including names of each part is shown in Fig 4.

In 2D experiment, the optical lens power of 21 lenses are from -10D and 10D in 1D steps, which were named A through U. They have the same diameter and curvature radius of the back surface, but the curvature radius of the front surface depends on the lens power. Also, the curvature radius of the lens periphery of the front surface, the diameter of the optical zone, which is the area displaying the required correction lens power, and the center thickness are

different depending on lens. Therefore, the measurement range is calculated from the optical zone diameter and the curvature radius of the front surface.

In 3D experiment, we adopted 5 lenses which have the specialized characteristics. It is whether the centers of curvature radius on the front and back surface are same or not. Accordingly, the thicknesses are adjusted. The specifications of the sample lenses are shown in Table 2.
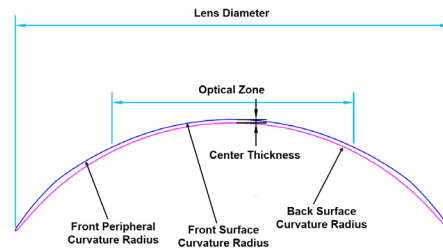

Figure 4: Structure of a typical contact lens.

Table 2: Specifications of the sample lenses for 3D measurement.

Sample lens	Front Surface Curvature Radius [mm]	Back Surface Curvature Radius [mm]	Lens Diameter [mm]	Center Thickness [mm]
A	7.92	7.82	10.0	0.10
B	7.97	7.82	10.0	0.15
C	7.92	6.67	10.0	1.25
D	6.77	6.67	10.0	0.10
E	7.92	6.67	10.0	0.054

3 EXPERIMENTAL RESULTS

3.1 2D Shape Measurement

In 2D measurement study, shape, curvature radius and thickness of sphere lenses were evaluated. Figure 5 shows (a) design drawing of the lens as a representative sample and (b) its measurement results. In Fig. 5 (a), within 5.77 mm of the optical zone, the curvature radius was 6.68 mm (Designed FS1) whereas in the peripheral part, it was 7.20 mm (Designed FS2). The curvature radius of the back surface had a constant 6.67 mm (Designed BS). In Fig. 5 (b), 3 trial measurements were conducted in the vertical rotation angle, ranging from -35° to 35° in 5° steps. Compared with the design value in Fig. 5 (a), the same transition of the curvature radii was observed in the OCT measurement results in Fig. 5 (b). That is, Designed FS1 and FS2 well matched with the result (FS) 1-3 on optical zone and peripheral part,
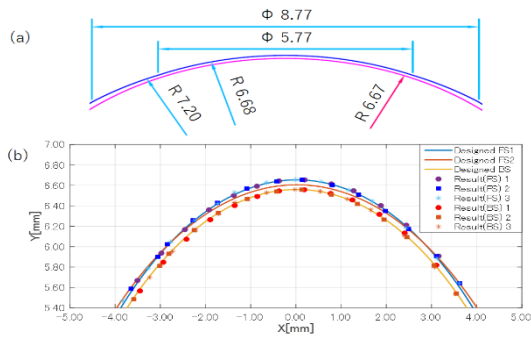
Figure 5: (a) Drawing for lens design and (b) measurement results of the front and back surfaces with OCT of sample lens K (Power 0.00D).

respectively. When the curvature radius was estimated by the circle approximation of the OCT results, the curvature radii of the back surface was 6.71 mm, and for the optical zone and peripheral part of the front surface, they were 6.70 mm and 7.21 mm, respectively.

Figure 6 shows the result of the thickness distribution compared with the designed values. The thickness is shown at each vertical rotation angle, which ranges from -30° to 30° in 1° steps. The root mean square error (RMSE) was 5.33 µm against the distribution of the designed thickness. The ISO standard is only applicable to the central part and the tolerance limit for the design value is within $\pm$ 0.02mm. Even though the experimental error of 5.33 µm takes into account the thickness of the peripheral part, it was remarkably small compared with the criteria value.

The curvature radius estimated by our OCT was evaluated in comparison with Plu Apex. Figure 7 shows the measured curvature radius results of 21 sample lenses. Compared with the designed values, with respect to the front surface, the errors from the designed values tend to increase as the curvature radii become large in both of our OCT and Plu Apex results.

In our OCT results, the error is large in the sample lens U, which has the largest difference in the curvature radii between the front and back surfaces. That is, since there is a big difference of incident angles on both surfaces, the intensity of the vertically reflected light measured within N.A. is weaker than that of a lens with smaller difference in curvature radius. Thus, this algorithm affects the measurement results of the curvature radius because it determines the measurement point based on the interference intensity ratio between the front and back surfaces. On the back surface, both devices caused large errors on the same lens and their tendencies were opposite.
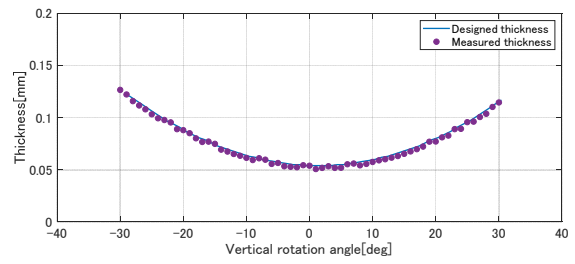

Figure 6: Thickness distribution of sample lens N (Power -3.00D).
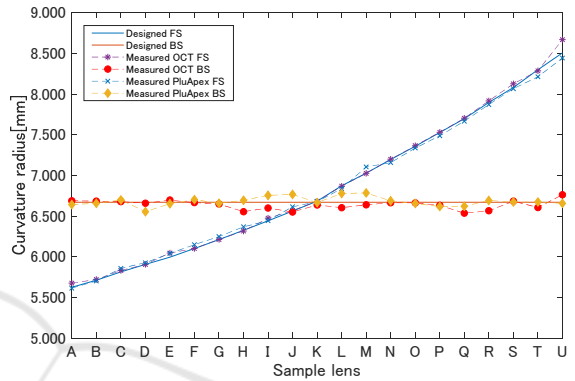

Figure 7: Estimation of curvature radii from our OCT and Plu Apex for sample lenses.

easuring the back surface shape, the lens was turned over to measure the front surface shape. On the other hand, our OCT can simultaneously measure front and back surfaces.

Here, analysis of results of Plu Apex and our OCT was performed by using Bland-Altman analysis. Regarding the front surface, the 95% limits of agreement (LoA) was from -0.77% to -2.09% and the correlation coefficient was 0.57, indicating a proportional bias. And Plu Apex and the developed OCT were compatible with each other on the front surface results. On the other hand, regarding the back surface, the error was large in the sample H to J, L and M, but there was no systematic bias (LoA was from -2.22% to -4.37%). Since there was no systematic bias, the Minimal Detectable Change (MDC) was 0.178 mm with 95% confidence interval (CI) due to the random error. Therefore, if the error is within 0.178 mm, the result is a measurement error. It is large for inspection of contact lens. This mainly came in the sample H to J, L and M results. Since CLs are manufactured with contact gauge check, if the measurement position is compatible with the designed values, the measured lens is considered as a good product. That is, there is an error factor outside the measurement range of contact gauge. Since the standard deviation (SD) is calculated by using the

difference of the measured results from both devices, SD became large and the MDC calculated using SD accordingly became large. This shows that it is possible to measure a wider range than contact gauge, and measure the part that could not be measured by the current method.

3.2 3D Shape Measurement

In 3D experiment, the front and back shape of CL were simultaneously measured. The measurement range was set to 1.53°, 3.60°, 5.66°, and 7.72° in consideration of the optical zone where the correction power is designed. The curvature radius and thickness were evaluated. Table 3 shows the curvature radius of each lens, and Table 4 shows the center coordinates, respectively.

Regarding the front curvature radius of lens A and lens B, lens A was 7.68 mm (error rate: 3.0%) and lens B was 7.71 mm (error rate: 3.2%). On the other hand, the back surface is 7.49 mm for lens A (error rate: 4.2%) and 7.51 mm for lens B (error rate: 4.0%). An error of about 0.3 mm was observed on the both surfaces compared with the design values. Here, in order to discuss the error, the simulation using known curvature radius was performed under the same conditions as this measurement. In other words, the measurement environment was reproduced and the results were evaluated. As a result, the error rate equivalent to the measurement result by OCT was obtained when 0.7% noise was added to the ideal value of the sphere. And then, the error rate was 11.0% as a result of applying the correction to the simulation data. In other words, a maximum error rate of 11.0% can occur in this measurement environment. Since the measurement range is narrow against the entire sphere, the error was occurred by applying the sphere fitting. Compared with the results, both A and B lenses had good results in this measurement environment. Regarding the lens C, the curvature radius of the front surface was 8.01 mm (error rate: 1.1%), and the radius of curvature of the back surface was 6.96 mm (error rate: 4.3%). Compared with lens A and lens C, it had a smaller difference from the design value on the both surfaces. Also, as the feature, the error of the lens A is on the minus side, but the error of the lens C is on the plus side. This was affected by the displacement (fixing method, humidity, etc.) due to the measurement environment. Since the lens C has a large thickness, it is not easily attached by deformation. Regarding the lens D, the curvature radius of the front surface was 6.84 mm (error rate: 1.0%), and the back surface was 6.93 mm (error rate: 3.9%). Compared with lens A, the result

of lens D was better. Since the lens D has a smaller curvature radius than the lens A, it is possible to measure data in a deeper direction to the center, which was led to good results when fitting the sphere. Finally, the lens E had a curvature radius on the front surface of 6.77 mm (error rate: 14.5%) and the back surface is 6.74 mm (error rate: 1.0%). The error rate on the lens surface was the largest. Compared with lens C, Table 4 shows that the center coordinates of the lens surface were shifted in the optical axis direction, and the tendency was that they are vertically incident on the back surface. Therefore, it is considered that the lens E had a larger error rate on the lens surface than the lens C, but the lens back surface was smaller. This result suggests to distinguish that the centers of the front and back are same or not.

Regarding the thickness, Figure 8 shows the thickness distribution of lens D. Since the center coordinates of the both surfaces are the same, the thickness is uniform. As shown in Figure 8, the uniform thickness were obtained. Compared with the design value, the difference was 6 μm. Also, Table 5 shows the average thickness and standard deviation of each lens. As shown in this Table 5, accurate measurement was possible. Regarding the lens C, which has the largest error and standard deviation from the design value, an error of 53 μm was occurred because the lens thickness was set to be so thicker lens that is not used for normal vision correction in order to match the center coordinates of the both surfaces. Since this lens is thick, the internal reflections affected to the result. The thickness result verified highly accurate measurement even when compared with the resolution of 10.1 μm of this OCT.

Table 3: The results of each curvature radius.

	Front surface[mm]	Back surface[mm]
A	7.68	7.49
B	7.71	7.51
C	8.01	6.96
D	6.84	6.93
E	6.77	6.74

Table 4: The results of the center coordinates.

	Front surface [mm]			Back surface [mm]		
	x	y	z	x	y	z
A	0.00	0.01	0.28	0.16	0.06	0.03
B	0.00	0.02	0.01	0.05	0.00	0.05
C	0.25	0.00	0.00	0.01	0.01	0.02
D	0.50	0.00	0.01	0.09	0.00	0.00
E	0.13	-0.01	0.01	0.08	0.00	0.00

Table 5: The results of the thickness.

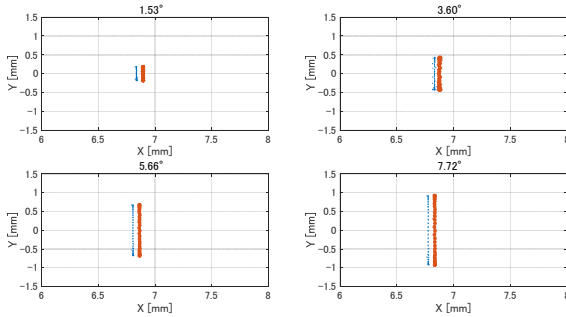|	A	B	C	D	E
Design value [mm]	0.10	0.15	1.25	0.10	0.054
Average value [mm]	0.088	0.143	1.197	0.094	0.055
Std [mm]	0.013	0.008	0.020	0.003	0.008

Figure 8: Lens D's thickness distribution for each measurement range. '*' is the front surface. And '.' is the back surface.

4 CONCLUSIONS

In this paper, we proposed the 2D and 3D measurement algorithms for the real front and back curved surfaces of CL. Since 2D uses the interference intensity ration of the front and back surfaces, it takes time to measure, and although 3D has a limited measurement range, two measurement algorithms that can measure both shapes of transparent objects have great advantage.

Regarding 2D measurement algorithm, changes in curvature radius and a wide range of thickness distributions can be measured. In recent years, peripheral shape of CL is an important issue for the design of new lenses, such as CL for myopia control. The fact that OCT provides quantitative measurement is advantageous as a CL shape measuring device. Also, since the front and back surfaces can be measured simultaneously, it is possible to analyze the misalignment between the both surfaces. This is important for small optical lenses such as CLs. For lens curvature radius, circle approximation results from the obtained shape coordinates were equivalent to those of Plu Apex. Nevertheless, our OCT device is more superior because it can measure lens front and back surfaces simultaneously.

Regarding 3D measurement, the simulation was performed under the same conditions and compared with the error rate of experimental results. Compared with the simulation data, it was confirmed that the error rate became smaller and the accuracy was satisfied in this measurement environment. In addition, the thickness was sufficiently accurate compared with the resolution of this OCT. The next step is to evaluate toric-shaped contact lens.

From these results, 2D and 3D algorithm were able to solve the problem of the shape measurement device, which is the measurement of transparent object, by measuring the front and back surfaces at the same time. Therefore, this algorithm can be applied to the medical field such as the ophthalmology field. For example, it is an eyeball shape measurement. By using this method, information such as the corneal shape of the front and back surfaces, thickness and the center coordinates of the curvature radius can be obtained. Also, it can measure non-cylindrical shapes such as keratoconus for eye diseases in which the cornea protrudes (D. Fadel 2018). In addition, it can be applied not only in the medical field but also in the industrial field. Nowadays, small lenses such as mobile phone camera lenses is frequently used. It is also possible to evaluate the misalignment of the front and back surfaces, which is applicable to the inspection of such lenses. This is an advantage of simultaneous front and back measurement. Simultaneous measurement of the shapes of front and back curved surfaces of transparent bodies such as CL provides a new measurement possibility for the industry.

REFERENCES

B. J. Coldrick, C. Richards, K. Sugden, J. S. Wolffsohn, and T. E. Drew, "Developments in contact lens measurement: A comparative study of industry standard geometric inspection and optical coherence tomography," Contact Lens Anterior Eye, 270-276 (2016).

D. Luo, L. Qian, L. Dong, P. Shao, Z. Yue, J. Wang, B. Shi, S. Wu, and Y. Qin, "Simultaneous measurement of liquid surface tension and contact angle by light reflection," Opt. Express, Vol. 27, No. 12, 16703-16712 (2019).

F. Drouet, C. Stolz, O. Laligant, and O. Aubreton, "3D reconstruction of external and internal surfaces of transparent objects from polarization state of highlights," Opt. Lett., 39 (10):2955-8 May (2014).

K. Saeki, D. Huyan, M. Sawada, Y. Sun, A. Nakamura, M. Kimura, S. Kubota, K. Uno, K. Ohnuma and T. Shiina, "Measurement algorithm for real front and back curved surfaces of contact lenses," Appl. Opt. 59, No. 29 (2020).

N. Tanno, S. Kishi : "Optical Coherence Tomographic Imaging and Clinical Diagnosis," Medical Imaging Technology, Volume 17: 3-10 (1990).

P. Massatsch, F. Charriere, E. Cuche, P. Marquet and C. D. Depeursinge, "Time-domain optical coherence tomography with digital holographic microscopy,"Appl.Opt. 44, 1806-1812 (2005).

K. Hibino, Bozenko F. Oreb, Philip S. Fairman, and Jan Burke, "Simultaneous measurement of surface shape and variation in optical thickness of a transparent parallel plate in wavelength-scanning Fizeau interferometer," Appl. Opt. 43, 1241-1249 (2004).

H. C. Cheng and Y. C. Lin, "Simultaneous measurement of group refractive index and thickness of optical samples using optical coherence tomography,"Appl.Opt. 49, 790-797 (2010).

T. Shiina, Y. Moritani, M. Ito and Y. Okamura, "Long-optical-path scanning mechanism for optical coherence tomography,"Appl. Opt. 42, 3795-3799 (2003).

D. Fadel, "The influence of limbal and scleral shape on scleral lens design," Contact Lens and Anterior Eye., 41, 321-328 (2018).